Received 21 July 2023; revised 23 September 2023; accepted 25 September 2023. Date of publication 4 October 2023; date of current version 26 October 2023.

Digital Object Identifier 10.1109/OJAP.2023.3321932

A Global Optimization Method for Wideband and Small Supergain Arrays Design Using Artificial Neural Network

ABDELLAH TOUHAMI (Student Member, IEEE), SYLVAIN COLLARDEY, AND ALA SHARAIHA (Senior Member, IEEE)

Univ. Rennes, CNRS, Institut d'Electronique et des Technologies du numéRique, UMR 6164, 35000 Rennes, France

CORRESPONDING AUTHOR: A. TOUHAMI (e-mail: abdellah.touhami@univ-rennes.fr)

This work was supported by the French National Research Agency (ANR) through the COMET-5G Project under Contract ANR-19CE24-0010.

ABSTRACT This paper introduces an efficient approach for compact, wideband and supergain arrays design using artificial neural network (ANN) based optimization. The proposed method optimize at the same time the distance inter-elements of the array antenna, its input impedance as well as its directivity. Such global optimization considerably improves the performances of superdirective arrays in terms of gain, bandwidth and efficiency. The proposed method is used afterwards to synthesize a three-elements array using two different unit elements. The comparison of the achieved performances and the Harrington limit reveals that the developed antennas can be qualified as supergain antennas. To our knowledge, this is the first demonstration of a wideband supergain array with more than two elements in the open literature. To validate the results, a prototype was manufactured and measured. The measurements show that the antenna has a wide impedance bandwidth of 22.6 %, a peak directivity of 8.3 dBi and a total efficiency greater than 80%.

INDEX TERMS Superdirective array, supergain array, parasitic array, directivity, artificial neural network, optimization algorithm.

I. INTRODUCTION

THE RECENT trends towards compact and connected objects technologies, imposes a growing demand for miniaturized, directive, wideband and efficient antenna systems. However, miniaturizing an antenna while maintaining a high performances is a challenging and difficult task. In [1], R.F. Harrington have demonstrated that the directivity of an antenna confined in a radian sphere of radius r, can reach a peak of $M^2 + 2M$, where $M = kr$ (electrical size) and $k = \frac{2\pi}{\lambda}$ (wavenumber). Consequently, as the electrical size of the antenna decreases, its directivity drops and its radiation tends to have an omnidirectional pattern which lead to radiations in unwanted directions.

To address this issue, several works have been conducted on compact superdirective array. Such antenna system has the advantage of transforming the omnidirectional radiation patterns of electrically small antennas (ESAs) to a very directive one.

In [2], Uzkov have shown that with an appropriate adjustment of the excitation, amplitude and phase, the end-fire directivity of N-tightly spaced antennas can approach N^2. Since then, various design methodology have been developed in the open literature. Most notably [3], [4] and [5]. All these methods, use the same technique: optimizing the directivity by optimizing the excitation for a fully driven case or the parasitic loads for a parasitic configuration.

In [3], the authors have studied theoretically and experimentally the superdirectivity on a two monopole-based array. Providing the optimal excitation, it was shown that the array achieves a superdirectivity for tight separation distances. However as the number of element increase and/ or the inter-element distance decreases, the array becomes very sensitive to small perturbation on the excitation and therefore a high accuracy on both excitation magnitude and phase is required. Such increasing precision make the design of the array feed network the most difficult part in superdirective array design.

To overcome this problem, parasitic superdirective array are widely studied. In this configuration we don't really need a feed network, since only one element is excited, while the parasitic elements are either loaded, shorted or open circuited [6], [7], [8], [9], [10], [11]. In [4] and [8], the authors have introduced a simple methodology to calculate the optimal loads for parasitic elements using their active impedance. However the array efficiency as well as its impedance bandwidth drops dramatically due to the very low input resistance. The authors highlighted that the synthesis of such array subject to a trade-off between compactness, efficiency and directivity.

Indeed, parasitic superdirective arrays are often qualified as impractical due to their low efficiency, very low gain, high input VSWR and narrow bandwidth [12]. This performances become even worse for configuration with intense mutual coupling, such as array with small separation distance or dense array. The reason behind the efficiency degradation for superdirective array is that when the mutual coupling between elements becomes intense, the radiation resistance decreases rapidly and the ohmic losses become dominant. Nevertheless the author in [12] have demonstrated that with the choice of a high input free space resistance antenna as unit element and an optimal separation distance, we can achieve higher efficiency. To do so, the authors have used a multi-arms monopole over a large ground plane to increase the antenna feed point impedance. Afterwards they used it as a unit element to design an efficient superdirective array, but over a narrow bandwidth. In fact, till now, the design of an efficient and wideband superdirective array still a big challenge especially when the inter-element distance of the antenna array is small (compact array) or for multi-elements array with number of elements greater than 2.

To address these issues, in this paper we propose an efficient synthesis method for compact, wideband and efficient superdirective arrays design using an artificial neural network (ANN) based optimization. The proposed method takes into account the optimization not only of the array directivity as in the literature, but also the array input impedance as well as the separation distance between its elements. Such global optimization yields to a wideband and efficient superdirective array, or simply wideband supergain array, which is not possible with mono-objective optimization procedure presented in the state of art.

Recently, ANN are known as a powerful modeling tool and have been widely studied and used in the design and optimization of RF circuits such as filters [13], [14], sensor [15], loop antenna [16], dual and multi-band antennas [17], [18], [19], [20], [21], ultra wideband antenna [22], antenna in dielectric environment [23], dielectric resonators [24], [25], base station antenna tilting [26], Yagi Uda antenna [27] and array antennas [28], [29], [30], [31], [32], [33], [34]. Through a training process, the ANN are capable to learn, map and generalize complex nonlinear relationship between synthesis variables and their corresponding electromagnetic (EM) responses. Also, they are capable to incorporate the real radiating properties and the coupling effects in the synthesis process without increasing the complexity of the model which can be used for a reliable prediction over a wide range of input parameters [13], [14], [15], [16], [17], [18], [19], [20], [21], [22], [23], [24], [25], [26], [27], [28], [29], [30], [31], [32], [33], [34].

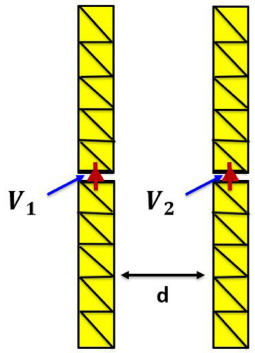

FIGURE 1. Fully driven array based on strip dipole.

Intuitively other techniques such as stochastic algorithms implemented in EM solvers can be used to performs such global optimization. However the intense mutual coupling of such array lead to inaccurate solutions and consequently to the non convergence of the optimization. Hence the choice of the ANN-based optimization.

To explain the synthesis methodology, the paper is organized as follows. A brief formulation of the problem is given in Section II. Section III addresses the challenges and motivations for the ANN-based optimization. The application on a three-elements arrays is presented in Sections IV and V. Simulation are practically verified in Section VI. Finally the paper is concluded in Section VII.

II. PROBLEM FORMULATION

A. FULLY DRIVEN ARRAY

Let consider a fully driven array of two strip dipoles (Fig. 1), where the current density $J(r)$ is excited with two voltage sources V_1 and V_2. This density can be expanded in a local basis functions ψ_n as follows [35], [36]:

$$J(r) \simeq \sum_{n=1}^{N} I_n \psi_n(r) \tag{1}$$

where I_n are unknown current expansion coefficients and N is the basis function number (with $N >>> 1$).

The Electric Field Integral Equation (EFIE) gives:

$$E(r) = -\mathrm{j}Z_0 k \int_{\Omega} \left(\mathbf{I_d} + \frac{\nabla\nabla\cdot}{k^2} \right) J(r') \frac{\mathrm{e}^{-\mathrm{j}kR}}{4\pi R} \, \mathrm{d}S \tag{2}$$

with $\mathbf{I_d}$ being the identity matrix, Z_0 the vacuum impedance, k the wave number and $R = |r - r'|$ the observation point.

A standard method of moment (MoM) implementation of the EFIE dictates:

$$[\mathrm{V}] = [\mathrm{Z}].[\mathrm{I}] \tag{3}$$

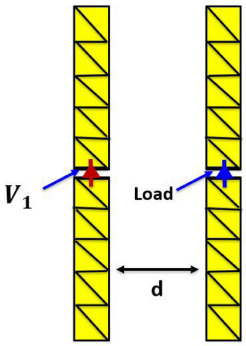

FIGURE 2. Parasitic array based on strip dipole.

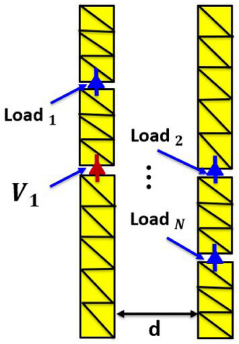

FIGURE 3. Parasitic strip dipole based array with N loads.

where [V] is a $N \times 1$ vector of voltage excitation coefficients, [**I**] is the $N \times 1$ vector of current expansion coefficients I_n and [Z] is the $N \times N$ MoM impedance matrix. Inverting the equation (3) we can deduce the expansions coefficients as follows:

$$[\mathrm{I}] = [\mathrm{Z}]^{-1}.[\mathrm{V}] \tag{4}$$

B. ANTENNA DIRECTIVITY

Substituting (4) in (1), we can deduce the current density $J(r)$ on the dipole based array and thus its radiation as follows:

$$F(\hat{r}, \hat{e}) = \lim_{r \to \infty} \left\{ r e^{jkr} \hat{e} \cdot E(r) \right\}. \tag{5}$$

Hence the array directivity is:

$$D(\hat{r}, \hat{e}) = \frac{4\pi U(\hat{r}, \hat{e})}{P_{\mathrm{rad}}} \tag{6}$$

where

$$U(\hat{r}, \hat{e}) = \frac{1}{2Z_0} |F(\hat{r}, \hat{e})|^2, \text{ and } P_{\mathrm{rad}} = \int_{space} U(\hat{r})\, \mathrm{d}\Omega, \tag{7}$$

Therefore, by choosing the optimal separation distance **d** and adjusting the excitation V_1 and V_2 of each element, we can excite an optimal current density $J(r)$ that maximize the array directivity in a desired direction (θ_0, ϕ_0). In the open literature, several method can be used to calculate the optimal excitation coefficients [3], [4], [5].

C. PARASITIC ARRAY

Now, we consider a parasitic configuration (Fig. 2), in which the excitation port of the second element is loaded. The equation (4) becomes:

$$[\mathrm{I}'] = [\mathrm{Z} + \mathrm{Z}_{Load}]^{-1}.[\mathrm{V}'] \tag{8}$$

where Z_{Load} is the diagonal (assuming a lumped element) load impedance matrix. Hence, if we choose the appropriate load that ensure the equality between $[\mathrm{I}']$ in (8) and [I] in (4), we can achieve the same directivity as the fully driven array (at least at the optimization frequency). This equality can be ensured if the parasitic antenna is loaded by the opposite of its active impedance [8].

$$\mathrm{Z}_{Load} = -\mathrm{Z}_{active} \tag{9}$$

D. ANTENNA INPUT IMPEDANCE

Once the current distribution is found, the antenna input impedance can be determined using the ratio of the input port voltage to current as follows [37]:

$$\mathrm{Z}_{Input} = \frac{\mathrm{V}_{Input}}{\mathrm{I}_{Input}} \tag{10}$$

So, by adjusting Z_{Load} we can optimize not only the directivity but also the antenna input impedance.

E. MULTI-LOAD ANTENNA

In the above described case depicted in (Fig. 2), the loading matrix Z_{Load} has only one element in its diagonal. Now, let consider the case of a multi-load antenna (Fig. 3). All loads are considered as lumped elements. In this case, the diagonal load impedance matrix Z_{Load} has N-elements instead of one. That's gives more flexibility to optimize the directivity and the input impedance in a large frequency band.

III. DESIGN METHODOLOGY

As it's obvious, the array parameters in terms of directivity and input impedance depend mainly on the current distribution $J(r)$ of the antenna. This distribution in its turn depend on:

- The antenna geometry (e.g., shape, separation distance).
- The loading impedance matrix Z_{Load}.

Here, we don't consider any antenna shape optimization. So for a given unit element shape, if we choose an optimal separation distance, and if we adjust properly the loads impedance matrix, we can excite an optimal current density that gives a superdirective array with high input resistance. That's results in an efficient superdirective antenna or simply supergain antenna. To perform such multi-parameter optimization we propose an optimization approach based on artificial neural network (ANN). During this optimization, the ANN model will be used as a surrogate model and will be combined with a heuristic algorithm to search for the best separation distance between array elements as well as the optimal impedances of the embedded loads.

A. ANN MODEL

The proposed ANN model consists of two independent branches. The first one maps the relationship between the synthesis variables and the antenna input impedance, while the second relates the same synthesis variables to the antenna directivity. Here, the synthesis variables consists of the separation distance between array elements as well as the loads values (loading impedance matrix elements):

1) INPUT IMPEDANCE BRANCH

A direct approach to maps the relationship between the synthesis variables and the antenna input impedance is to set the former as the ANN input and the latter as its output. However, the strong sensitivity of the input impedance to the synthesis variables may leads to inaccurate prediction. To overcome this problem, in our case we divided the branch 1 into two parts (Fig. 4):

- *ANN Part:* This stage relates the separation distance and the frequency to the N port impedance matrix, Z_{Nport}.
- *Code Part:* In this stage we use the N port impedance matrix obtained from the output of the ANN part as well as load impedance values Z_{Load}, to compute the input impedance using the formulas (13) and (15).

2) DIRECTIVITY BRANCH

This branch maps the relationship between the synthesis variables and the antenna directivity in the end-fire direction ($\theta = 0, \phi = 0$). A classical technique to establish such relationship is to use a regression ANN model where the synthesis variable are in input and the directivity in the output. However, given the strong sensitivity of the problem a regression model is not suitable to achieve a high prediction accuracy. To overcome this issue we have transformed the regression problem into a classification one. In this case, an ANN-based classifier is used to classifies the synthesis variables into two classes (Fig. 5):

- *Superdirective Array Class* when the synthesis variables yield a directivity greater than the Harrington limit (definition of superdirective array).
- *Unsuperdirective Array Class* when the synthesis variables yield a directivity lower than the Harrington limit

For the Harrington limit H_0, it can be computed as follows [1]:

$$H_0 = 10.log_{10}\left(M^2 + 2M\right) \tag{11}$$

where M is the array antenna electrical size.

B. DATA GENERATION

In order to make the ANN model learn the complex non-linearity between the synthesis parameters in one hand and the EM responses in the other hand, it's necessary to use an appropriate training data. The idea is to collect an input-output database where we extract the EM responses of the

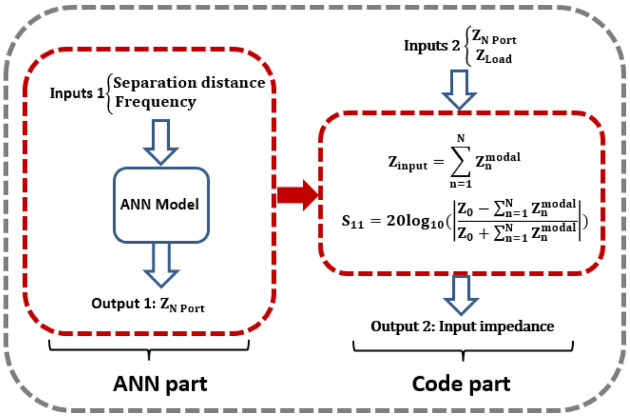

FIGURE 4. Proposed ANN model: Input impedance branch.

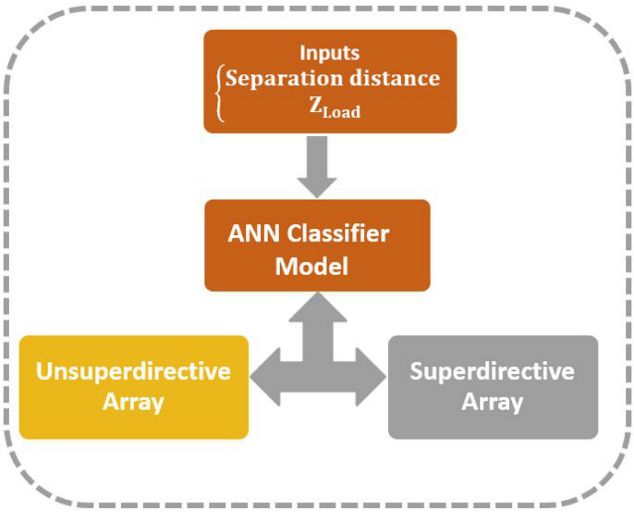

FIGURE 5. Proposed ANN model: Directivity branch.

array antenna to a random combination of synthesis variables. To do so, in our work we have combined the full wave simulation with analytical models of the antenna directivity and its input impedance as follows:

Let consider the example of the multi-load (N loads) antenna depicted in (Fig. 3). For a fixed separation distance **d**, the antenna total electrical field can be calculated as follows [38]:

$$\mathrm{E_{total}} = \sum_{n=1}^{N} \frac{\mathrm{I}_n.\mathrm{V_{oc}}}{1 + \mathrm{j}\cdot\gamma_n}.\mathrm{E(I_n)} \tag{12}$$

where I_n and γ_n are respectively eigen vectors and eigen values such as:

$$\left[\mathrm{Z_{Nport}} + \mathrm{Z_{Load}}\right]\mathrm{I_n} = (1 + \mathrm{j}\gamma_n)\left[\mathrm{R_{Nport}}\right]\mathrm{I_n} \tag{13}$$

$\mathrm{E(I_n)}$ is the field radiated when $\mathrm{I_n}$ excite the antenna ports, $\mathrm{Z_{Nport}}$ is the N port impedance matrix and $\mathrm{R_{Nport}}$ its real part. Once we determine the radiated field we can calculate

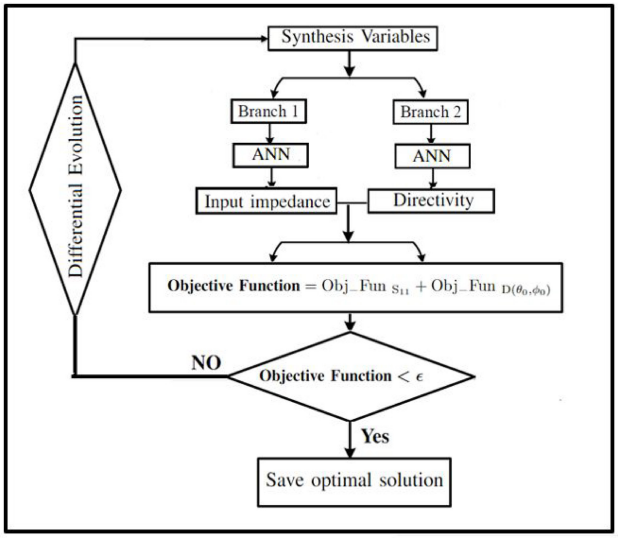

FIGURE 6. Optimization flowchart.

the antenna directivity, such as:

$$\mathrm{D}(\theta_0, \varphi_0) = 4\pi \cdot \frac{|\mathrm{E}_{\mathrm{Total}}(\theta_0, \varphi_0)|^2}{\int_0^{2\pi}\int_0^{\pi} |\mathrm{E}_{\mathrm{Total}}(\theta, \varphi)|^2 \sin\theta \mathrm{d}\theta \cdot \mathrm{d}\varphi} \tag{14}$$

For the antenna input impedance, it can be determined as follows [39]:

$$\mathrm{Z}_{\mathrm{input}} = \sum_{n=1}^{N} Z_n^{modal} \tag{15}$$

$$= -\left(\sum_{n=1}^{N} \alpha_n \left[\mathrm{I}_n(\mathrm{input})\right]^2\right)^{-1} \tag{16}$$

where α_n are modal weighting coefficients.

C. OPTIMIZATION FLOWCHART

Once the training and testing process is completed, the developed ANN model can be used afterwards instead of full wave EM solver to significantly speed up the optimization process. To do so, the trained ANN model is incorporated in an optimization loop, in which it's repeatedly called by a Differential Evolution algorithm [40] to search for the appropriate separation distance between array elements as well as the optimal set of internal loads (Fig. 6). The optimized synthesis parameters allows the excitation of an optimal current distribution over the antenna structure that yield in a wideband supergain array antenna.

To avoid adding constraints during the optimization on the antenna input reactance in one hand, and to ensure the antenna matching to the excitation source in the other hand, it's more convenient to optimize the antenna input reflection coefficient or the antenna input VSWR instead of it's input impedance such as:

$$\mathrm{S}_{11} = \frac{\mathrm{Z}_0 - \mathrm{Z}_{\mathrm{input}}}{\mathrm{Z}_0 + \mathrm{Z}_{\mathrm{input}}} \tag{17}$$

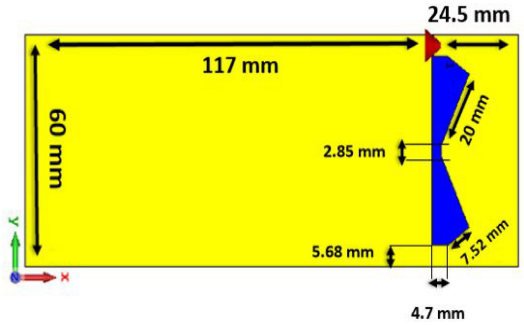

FIGURE 7. M-shaped loop antenna.

and

$$VSWR = \frac{1 + |S_{11}|}{1 - |S_{11}|} \tag{18}$$

where Z_0 is the source characteristic impedance.

D. ANN MODEL PROS AND CONS

In this subsection the ANN model pros and cons are summarized:

1) PROS

- The ANN incorporates the real radiating properties and the coupling effects in the synthesis process without increasing the complexity of the model.
- Speed up considerably the optimization process compared to the parametric study.
- Assign the appropriate load topology for each port (capacitance or inductance), which is not evident.

2) CONS

- Due to the intense mutual coupling, superdirective array presents a strong sensitivity to small perturbation on the synthesis variables. Since the ANN only approximates the relationship between the latter and EM response (according to the universal approximation theorem of ANN), it is possible that the solution given by the ANN is not the most optimal one.

IV. EXAMPLE I: M-LOOP ANTENNA BASED ARRAY

A. UNIT ELEMENT

The unit element used in this study is an M-shaped loop antenna printed on a Rogers RT5880 substrate. The antenna total dimensions are of $142 \times 60 \times 0.8$ mm^3 while those of the M-shaped loop are of 24.5×60 mm^2 (Fig. 7). The antenna presents a matched impedance bandwidth of 540 MHz between [1.66-2.2 GHz] (Fig. 8).

B. THREE ELEMENTS ARRAY

Using the above described antenna as a unit element we want to design a three-elements wideband supergain array using our proposed methodology. To make the problem more challenging, we want to operates the array in a low frequency band, namely the 5G NR n8 band between

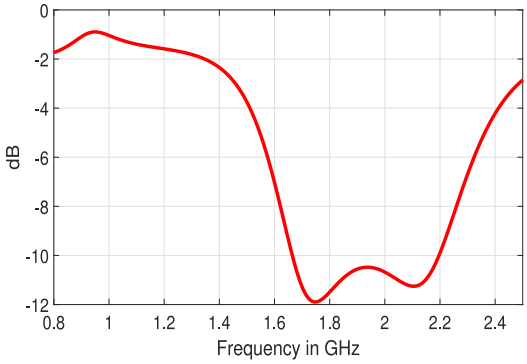

FIGURE 8. Antenna input reflection coefficient.

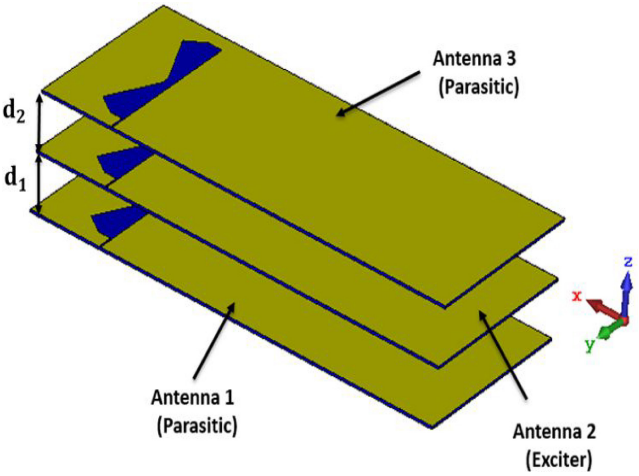

FIGURE 9. M-shaped loop antenna-based array.

[880 MHz-960 MHz] where the unit element is not matched (Fig. 8). Therefore, the synthesis task can be viewed as a miniaturization of the antenna array simultaneously with the optimization of its performances. (Fig. 9) shows the array geometry. It consists of three stacked antennas, where the central element denoted antenna 2 is excited while the peripheral ones, denoted respectively antenna 1 and 3 are parasitic.

C. INTERNAL LOADS SET UP

Following the above described optimization approach, four loads, denoted Load 1, Load 2, Load 3 and Load 4 have been inserted on the array antenna (Fig. 10). To avoid ohmic losses, only reactive loads are considered.

Once, the loads are inserted, the next step is to train the two branches of the ANN model.

D. DATA COLLECTION

Using the approach described in Section III-B, the antenna array with 5 port (one port for the excitation and the four remaining to be loaded) are simulated using a full wave simulation to extract the impedance matrix Z_{Nport} as well as

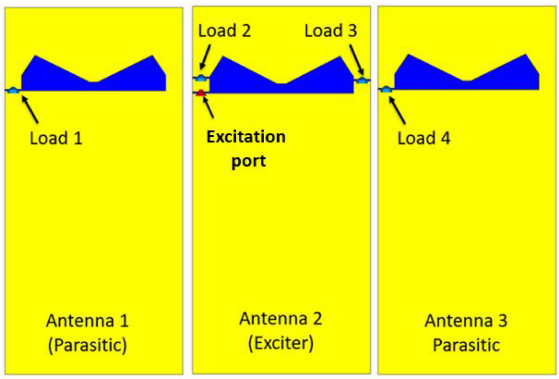

FIGURE 10. M-shaped loop based array: internal loads set up.

the radiated fields E_n, for different separation distances **d** between array elements.

For superdirective array the separation distance is $< 0.25\lambda$, where λ is the wavelength at the optimization frequency. Therefore the array antenna is simulated with a separation distance **d** in the range $[0.01\lambda–0.2\lambda]$ and a step of 0.04 λ. Here, λ is the wavelength at the 5G NR n8 band central frequency, 920 MHz. In overall, 6 simulations are needed for a uniform array and 36 for a non uniform one. Afterwards, all training data samples are easily generated using a post-processing in MATLAB, by a simple implementation of formulas (12)–(16).

E. TRAINING OF BRANCH 1

This part relates the separation distance and the frequency to the N port impedance matrix Z_{Nport}. Hence, for a given separation distance, we could determine the N port impedance matrix at each frequency point in the desired band. Since, the Z_{Nport} has complex parameters, two networks are used to compute respectively the real and the imaginary parts. Each network consists of an input layer, one hidden layer with 30 neurons and a sigmoïd activation function and an output layer with linear activation. Fig. 11 and Fig. 12, show the training mean square error of both network versus epochs. The two models exhibit the best validation performances respectively at 315^{th} and 955^{th} epochs. Thus we save the ANN weights and bias at these epochs.

F. TRAINING OF BRANCH 2

This branch classifies whether the array is superdirective or not based on the chosen synthesis variables. The ANN-based classifier model consists of an input layer, one hidden layer with 30 neurons and a sigmoïd activation function and an output layer with softmax activation function. Fig. 13 shows the training mean square error. The model exhibits the best validation performances at 16^{th} epoch. Thus we consider the ANN weights and bias at this epoch.

It should be noted that for both branches, the ANN model parameters (number of hidden neurons, the number

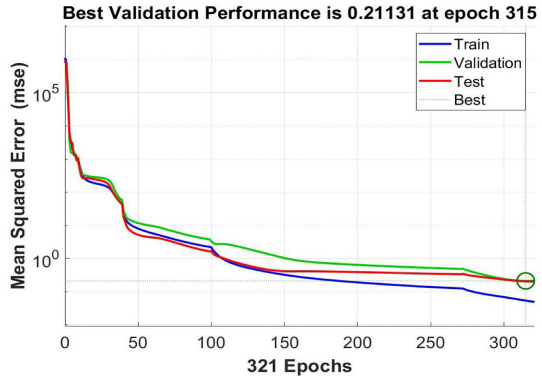

FIGURE 11. Training mean square error versus epochs: for the impedance matrix real part prediction.

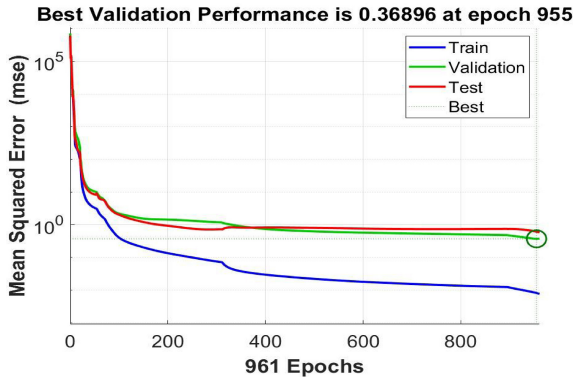

FIGURE 12. Training mean square error versus epochs: for the impedance matrix imaginary part prediction.

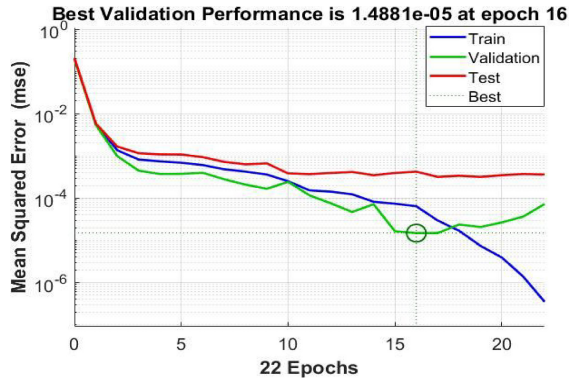

FIGURE 13. Branch 2 training mean square error versus epochs.

of hidden layers and the activation functions) are determined through trial and error (until the best training and validation performances are achieved).

G. OPTIMIZATION: UNIFORM ARRAY

Once, the training and testing process is completed, we launch an optimization using the optimization flowchart depicted in (Fig. 6). The yielded optimal synthesis parameters are depicted in Table 1.

With these optimized synthesis parameters, the antenna array achieves a peak directivity of 9.28 dBi, a front to back ratio of 11.34 dB (Fig. 14) and a –1 dBi directivity

TABLE 1. Optimized synthesis parameters.

	distance (λ)	Load 1	Load 2	Load 3	Load4
Optimized value	0.193	33 nH	3.6 pF	0.3 pF	0.4 pF

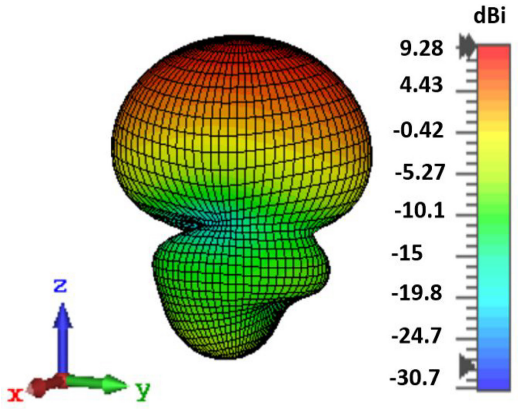

FIGURE 14. Optimization results: (a) 3D radiation pattern at 920 MHz.

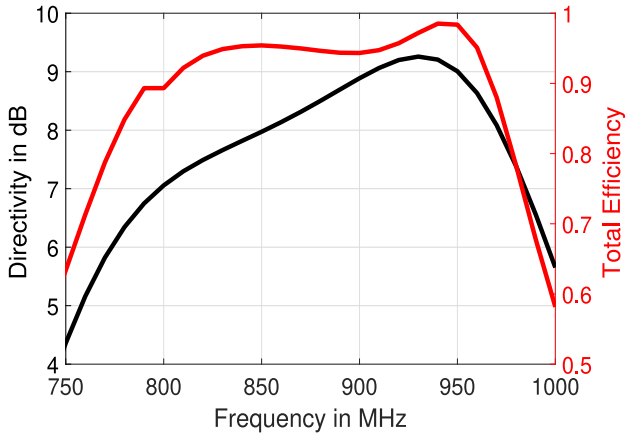

FIGURE 15. Optimization results: Directivity and total efficiency versus frequency.

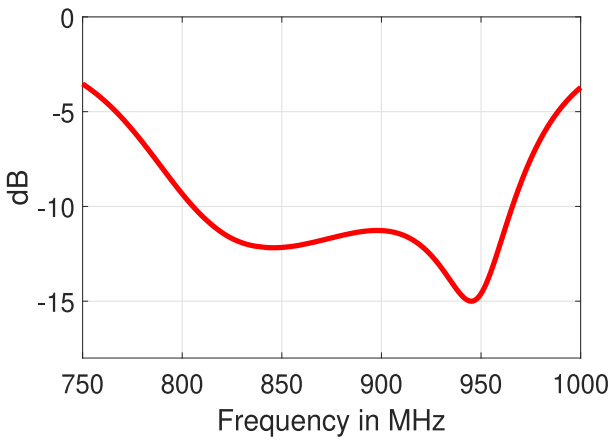

FIGURE 16. Optimization results: array input reflection coefficient.

bandwidth of 12.73% (Fig. 15). Furthermore, the array exhibits a total efficiency higher than 80% over a large bandwidth of 21.16%. Finally, the antenna is matched over a wide bandwidth of 16.87% (Fig. 16). Here, the center

TABLE 2. Optimized synthesis parameters.

d1	d2	Load 1	Load 2	Load 3	Load4
0.162 λ	0.193 λ	17 nH	2.6 pF	0.35 pF	0.4 pF

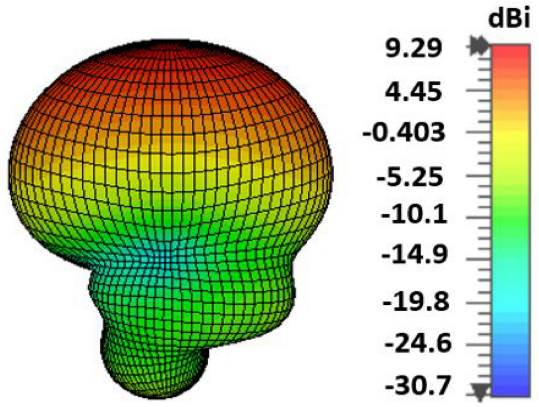

FIGURE 17. Optimization results:3D radiation pattern at 920 MHz.

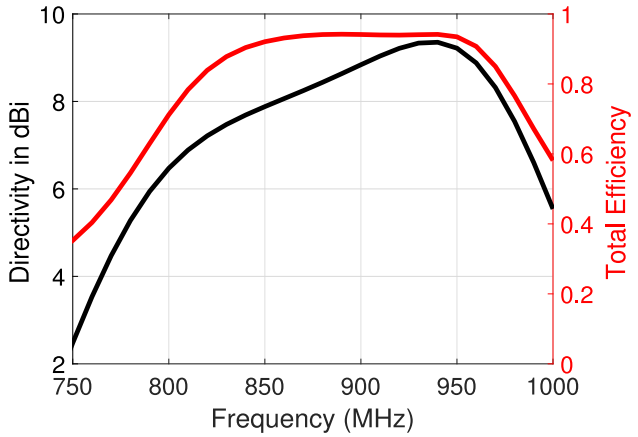

FIGURE 18. Optimization results: Directivity and total efficiency versus frequency.

frequency used to calculate the bandwidth percentage is 920 MHz (central frequency of the 5G NR N8 band).

H. OPTIMIZATION: NON-UNIFORM ARRAY

In this paragraph, we consider the case of a non-uniform array with different separation distances between its elements. The optimization gives the optimal synthesis parameters depicted in Table 2.

With these optimized synthesis parameters, the antenna array achieves a peak directivity of 9.29 dBi, a front to back ratio of 15.2 dB (Fig. 17) and a –1 dBi directivity bandwidth of 10.2% (Fig. 18). In addition, the array exhibits an efficiency bandwidth of 16.6% in which the total efficiency is higher than 80%. Also the antenna is matched over a wide bandwidth of 11.5% (Fig. 19).

It can be noted that the second design with non uniform separation distance is 8 % more compact than the case of a uniform array with comparable directivity and efficiency, a 5.3 % drops in impedance bandwidth and a better front to back ratio.

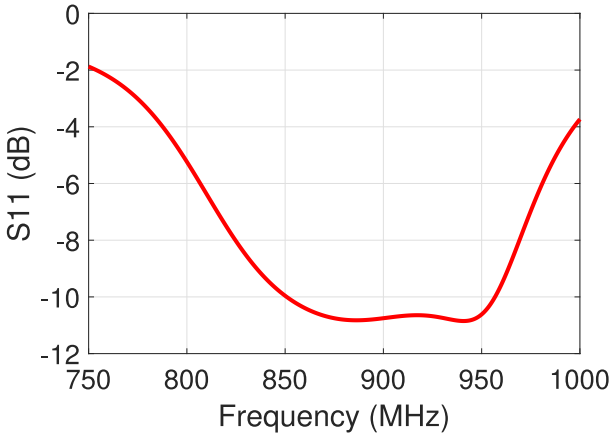

FIGURE 19. Optimization results: array input reflection coefficient.

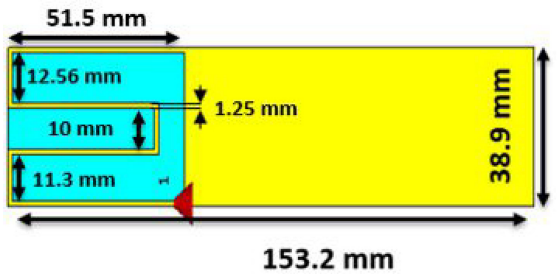

FIGURE 20. Folded monopole antenna.

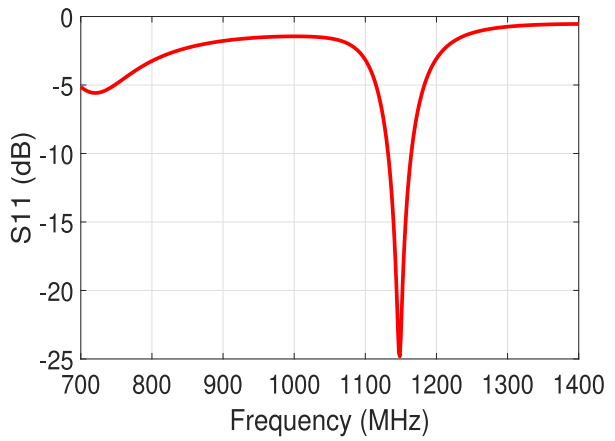

FIGURE 21. Antenna input reflection coefficient.

V. EXAMPLE II: FOLDED MONOPOLE BASED ARRAY

A. UNIT ELEMENT

The array unit element used in this example is a folded monopole printed on a Rogers RO4450B substrate of permittivity of $\epsilon_r = 3.7$ and loss tangent of $\tan\delta = 0.004$ [9]. The antenna dimensions are of $153.2 \times 38.9 \times 0.8$ mm^3 (Fig. 20). The antenna is matched over 32 MHz between [1.13–1.16 GHz] (Fig. 21).

B. THREE ELEMENTS ARRAY

Using the above unit element, a three elements array was synthesized and optimized in order to operates in the 5G NR n28 band between [758–803 MHz]. (Fig. 22) shows the array

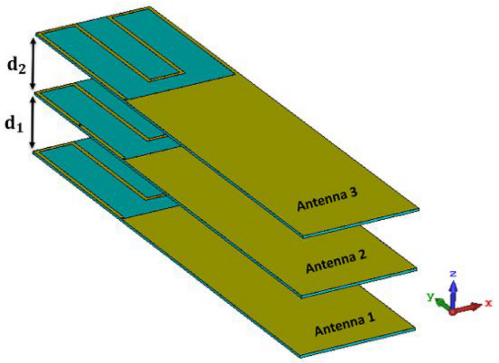

FIGURE 22. Folded monopole based array.

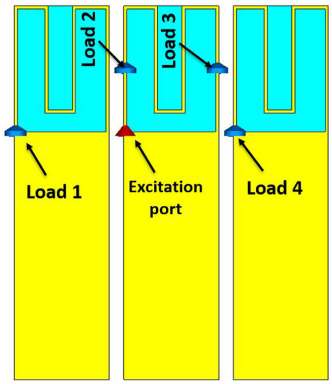

FIGURE 23. Folded monopole based array: internal loads set up

TABLE 3. OPTIMIZED synthesis parameters.

	d_1	Load 1	Load 2	Load 3	Load4
Optimized value	0.197λ	3.3 pF	1.1 pF	17.3 nH	0.4 pF

geometry. It's composed of three stacked antennas, where the central element (antenna 2) is excited and the peripheral ones (antenna 1 and 3) are maintained as parasitic elements.

C. INTERNAL LOAD SETUP

As in the first example, four loads are added on the antenna array as depicted in (Fig. 23). Also to avoid ohmic losses, only reactive loads are used.

Once, the loads are inserted, the next step is to train the two branches of the ANN model as described in Section IV.

D. OPTIMIZATION: UNIFORM ARRAY

First, we consider the case of uniform separation between the array elements ($d_1 = d_2$). The optimal synthesis parameters are depicted in Table 3.

With these synthesis parameters, the antenna array achieves a peak directivity of 9 dBi, a front to back ratio of 14.88 dB (Fig. 24) and a -1 dBi directivity bandwidth of 10.82% (Fig. 25). Also the array exhibits an efficiency bandwidth of 5.8% over which the total efficiency is higher than 80%. Moreover the antenna is matched over a bandwidth of 3.84% (Fig. 26). Here the center frequency used to calculate the bandwidth percentage is 780 MHz (central frequency of the 5G NR N28 band).

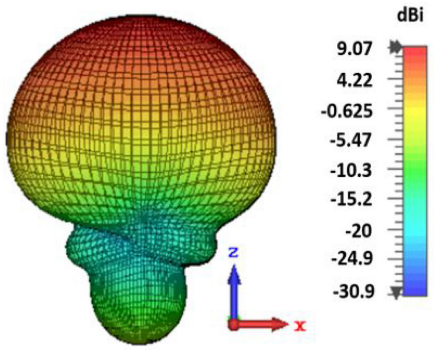

FIGURE 24. Optimization results: 3D radiation pattern at 780 MHz.

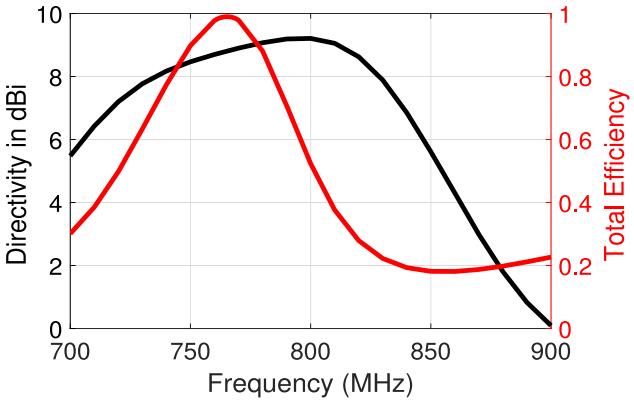

FIGURE 25. Optimization results: Directivity and total efficiency versus frequency.

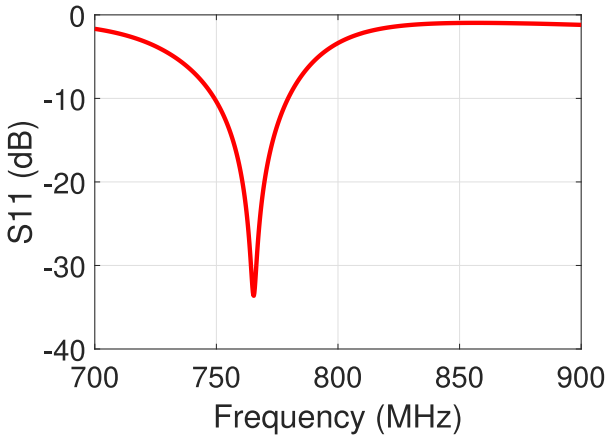

FIGURE 26. Optimization results: array input reflection coefficient.

E. OPTIMIZATION: NON-UNIFORM ARRAY

Here, we consider the case of a non-uniform separation between array elements ($d_1 \neq d_2$). The optimization yields the synthesis parameters depicted in Table 4.

With these optimized synthesis parameters, the antenna array achieves a peak directivity of 9 dBi, a front to back ratio of 16.83 dB (Fig. 27) and a –1 dBi directivity bandwidth of 8.13% (Fig. 28). Moreover, the array exhibits an

TABLE 4. Optimized synthesis parameters.

d1	d2	Load 1	Load 2	Load 3	Load4
0.188λ	0.169 λ	2.36 pF	1.88 pF	5.5 pF	0.534 pF

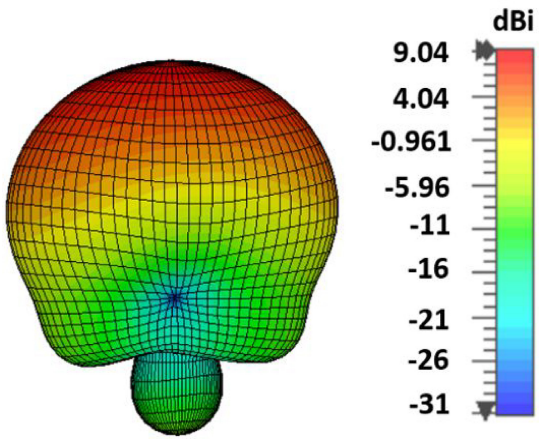

FIGURE 27. Optimization results: 3D radiation pattern at 780 MHz.

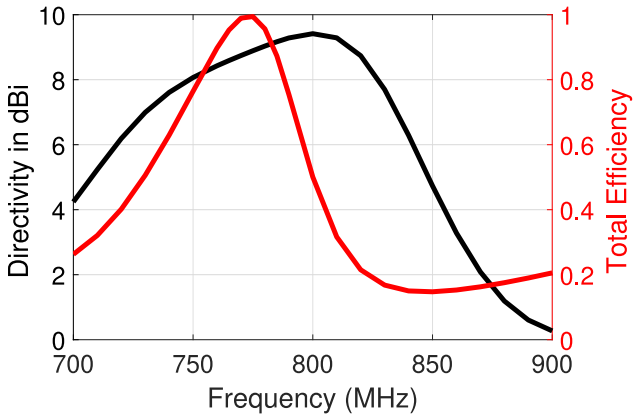

FIGURE 28. Optimization results: Directivity and total efficiency versus frequency.

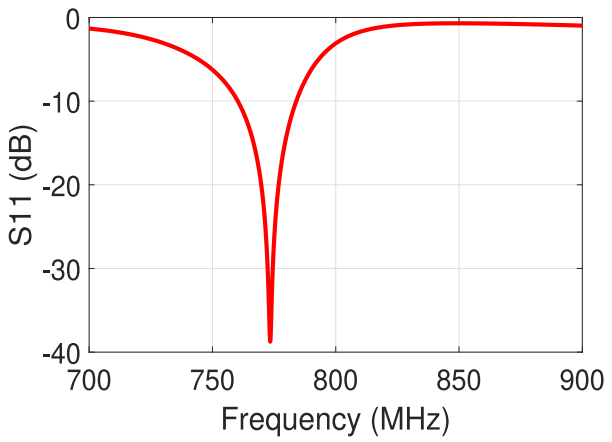

FIGURE 29. Optimization results: array input reflection coefficient.

efficiency bandwidth of 4.5% over which the total efficiency is higher than 80% and an impedance bandwidth of 3% (Fig. 29).

TABLE 5. Total time needed using our proposed ANN based approach.

	Uniform array	Non uniform array
Number of simulations	6 simulations	36 simulations
Data collection time	67.39 mins	404.42 mins
Model training time	0.833 min	4.6 mins
Optimization time	7.74 mins	8.85 mins
Total time	75.96 mins	417.8 mins

TABLE 6. Total time needed using parametric study.

	Uniform array	Non uniform array
Number of simulations	20 simulations	400 simulations
Total time	224.33 mins	4486.66 mins

Again, we can note that the second design with non uniform separation distance is 10% more compact than the case of a uniform array with comparable performances of directivity and efficiency, a 0.84 % drops in impedance bandwidth and a better front to back ratio.

F. STOCHASTIC ALGORITHM BASED OPTIMIZATION

Beside the ANN-based optimization, intuitively other techniques such as stochastic algorithms can be routinely used to performs such multi-criteria optimization. To do so, a global optimization over all the synthesis variables, separation distance and loads, is achieved using genetic algorithm implemented in CST microwave studio. However it doesn't converge after 497 solver run (almost 73 hours and 50 minutes). The non-convergence perhaps due to the intense mutual coupling (given the low separation distance) which lead to inaccurate solutions.

Another technique is to perform a parametric study over the separation distance **d** and optimizing the load values (at each distance) using formulas (12)–(16) combined with an optimization algorithm.

G. TIME DESIGN EFFICIENCY

To illustrate the design efficiency of the proposed method, in this paragraph we gives a comparison of the approximated time needed for the design of the antenna array of example II (presented in Section V) using ANN-based method (including data collection, model training, and optimization time) to that needed for a parametric study. During this latter, the separation distance is varied within the range $[0.01 - 0.2\lambda]$ with a step of 0.01λ. The used processor is an Intel Xeon CPU E5-2640 v3 @ 2.60GHz.

Tables 5 and 6 depict the total time required for each method. The comparison reveals that the time needed for the ANN-based method is 3 and 10 times lesser than that required for a parametric study for a uniform and non uniform array design respectively.

It should be noted that here the time needed for electromagnetic simulations is computed by multiplying the time needed for one EM simulation by the total number of used simulations.

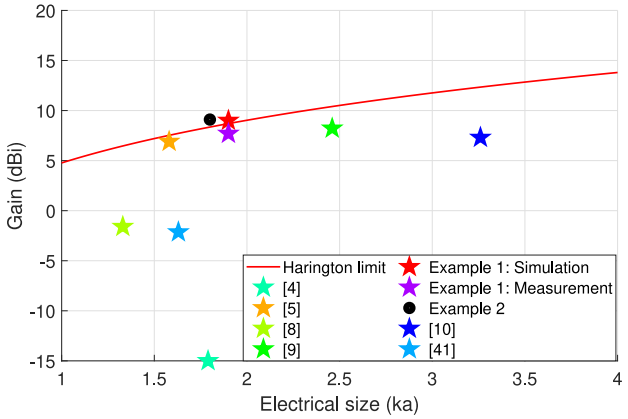

FIGURE 30. Gain comparison of our designs with respect to the state of art.

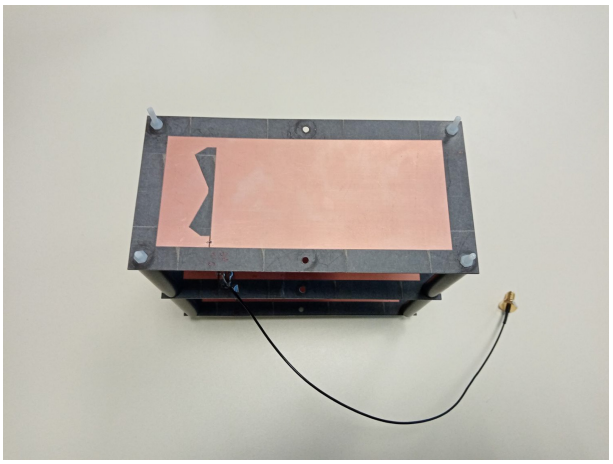

FIGURE 31. M-shaped loop based array.

VI. COMPARISON WITH THE STATE OF ART

To exhibit the usefulness of the proposed synthesis method, in this paragraph we compare the obtained performances of the above presented antennas to the designs presented in the open literature (Fig. 30). Similar to the directivity, the Harrington limit for gain, is computed using formula (11) considering a lossless case (efficiency of 100%). The comparison reveals that, our designs denoted Example 1 and Example 2 exhibit the best trade-off between compactness and gain compared to the state of art. Furthermore, both design are above the Harrington limit. Therefore they are indeed supergain antennas. To our knowledge, this is the first demonstration of a wideband supergain array with more than two elements in the open literature. It should be noted that all state of art designs with an infinite ground plane are excluded from this comparison since the computation of the electrical size $M = kr$ is not obvious, wherein $k = \frac{2\pi}{\lambda}$ is the wave number and r is the radius of the smallest sphere circumscribing the whole antenna.

VII. EXPERIMENTAL VALIDATION

A prototype of the M-shaped loop based array was fabricated and measured for results' validation (Fig. 31). (Fig. 32) shows the antenna measured input reflection coefficient in

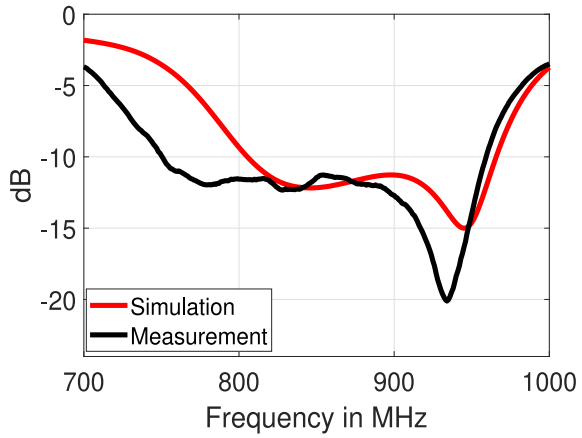

FIGURE 32. Measurement results: array input reflection coefficient.

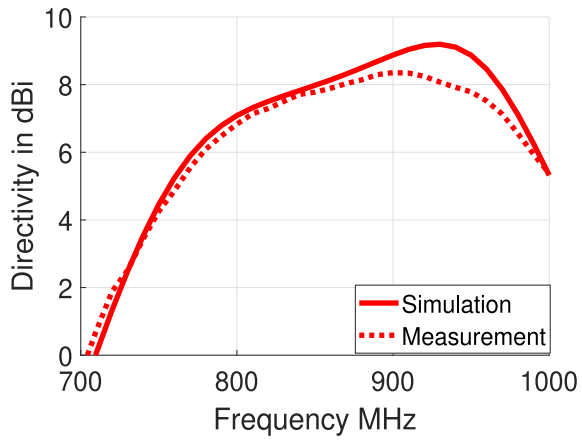

FIGURE 33. Measurement results: Directivity versus frequency.

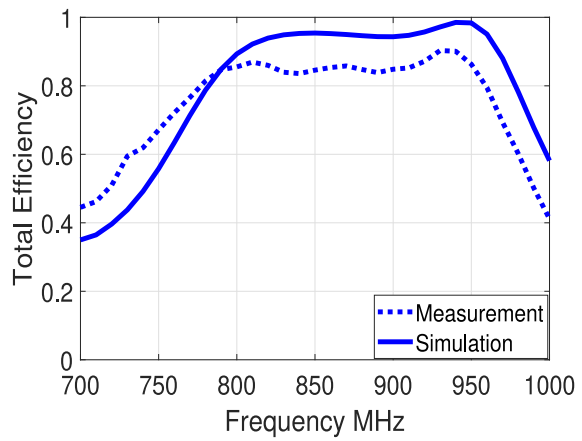

FIGURE 34. Measurement results: Total efficiency versus frequency.

dB. The measured impedance bandwidth is of 22.6 % while the simulated one is 16.87 %. This difference is due to the cable effects as well as the tolerances of the commercial SMD components. The antenna radiation properties were measured in a MVG Star Lab near-field based system. (Fig. 33) shows the measured directivity compared to the simulation. We can note that the both curves have the same

trend with a maximal level difference of 1 dBi. The noticed difference is mainly due to the chamber measurement accuracy which presents a peak accuracy of nearly $\pm 1.1 dBi$ in the frequency range [0.8–1 GHz] [42]. The measured total efficiency is depicted in (Fig. 34). As the simulation predicted, the antenna has a high total efficiency over the desired bandwidth. The small difference between simulation and measurement is due to the MVG Star Lab system accuracy as well as the internal resistances of the commercial SMD components.

VIII. CONCLUSION

This paper, introduces an artificial neural network based synthesis approach to address the issue of low efficiency, very low gain, and narrow bandwidth of superdirective arrays. The proposed ANN model consists of two parallel and independent branches. Once the synthesis variables are entered, it can simultaneously predict the array directivity and its input impedance from each corresponding branch. During the optimization process, the developed ANN model is repeatedly called by a Differential Evolution algorithm to search for the appropriate separation distance between array elements as well as the optimal set of internal loads. The optimized synthesis parameters allows the excitation of an optimal current distribution over the antenna structure that yield to a wideband supergain array antenna. The proposed method is utilized to design a three-elements supergain array with two different unit elements. To validate the results, a prototype with four SMD loads was manufactured and measured. Finally, it should be emphasized that the proposed methodology is applicable to synthesis array with much more elements.

REFERENCES

[1] R. F. Harrington, "On the gain and beamwidth of directional antennas," *IEEE Trans. Antennas Propag.*, vol. AP-6, no. 3, pp. 219–225, Jul. 1958.
[2] I. Uzkov, "An approach to the problem of optimum directive antennae design," *Acad. Sci.*, vol. 53, no. 1, pp. 35–38, 1946.
[3] E. E. Altshuler, T. H. O'Donnell, A. D. Yaghjian, and S. R. Best, "A monopole superdirective array," *IEEE Trans. Antennas Propag.*, vol. 53, no. 8, pp. 2653–2661, Aug. 2005, doi: 10.1109/TAP.2005.851810.
[4] A. Clemente, M. Pigeon, L. Rudant, and C. Delaveaud, "Design of a super directive four element compact antenna array using spherical wave expansion," *IEEE Trans. Antennas Propag.*, vol. 63, no. 11, pp. 4715–4722, Nov. 2015.
[5] H. Jaafar, S. Collardey, and A. Sharaiha, "Characteristic modes approach to design compact superdirective array with enhanced bandwidth," *IEEE Trans. Antennas Propag.*, vol. 66, no. 12, pp. 6986–6996, Dec. 2018, doi: 10.1109/TAP.2018.2874691.
[6] T. H. O'Donnell and A. D. Yaghjian, "Electrically small superdirective arrays using parasitic elements," in *Proc. IEEE Antennas Propag. Soc. Int. Symp.*, Jul. 2006, pp. 3111–3114.
[7] T. H. O'Donnell, A. D. Yaghjian, and E. E. Altshuler, "Frequency optimization of parasitic superdirective two element arrays," in *Proc. IEEE Antennas Propag. Soc. Int. Symp.*, Jun. 2007, pp. 3932–3935.
[8] A. Haskou, A. Sharaiha, and S. Collardey, "Design of small parasitic loaded superdirective end-fire arrays," *IEEE Trans. Antennas Propag.*, vol. 63, no. 12, pp. 5456–5464, Dec. 2015.
[9] M. Hammoud, A. Haskou, A. Sharaiha, and S. Collardey, "Small end-fire superdirective folded meandered monopole antenna array," *Microw. Opt. Technol. Lett.*, vol. 58, no. 9, pp. 2122–2124, Sep. 2016.
[10] O. S. Kim, S. Pivnenko, and O. Breinbjerg, "Superdirective magnetic dipole array as a first-order probe for spherical near-field antenna measurements," *IEEE Trans. Antennas Propag.*, vol. 60, no. 10 pp. 4670–4676, Oct. 2012.
[11] S. Lim and H. Ling, "Design of electrically small Yagi antenna," *Electron. Lett.*, vol. 43, no. 5, pp. 3–4, Mar. 2007.
[12] S. R. Best, E. E. Altshuler, A. D. Yaghjian, J. M. McGinthy, and T. H. O'Donnell, "An impedance-matched 2-element superdirective array," *IEEE Antennas Wireless Propag. Lett.*, vol. 7, pp. 302–305, 2008.
[13] C. Zhang, J. Jin, W. Na, Q.-J. Zhang, and M. Yu, "Multivalued neural network inverse modeling and applications to microwave filters," *IEEE Trans. Microw. Theory Techn.*, vol. 66, no. 8, pp. 3781–3797, Aug. 2018.
[14] H. Kabir, Y. Wang, M. Yu, and Q.-J. Zhang, "Neural network inverse modeling and applications to microwave filter design," *IEEE Trans. Microw. Theory Techn.*, vol. 56, no. 4, pp. 867–879, Apr. 2008.
[15] H. Acikgoz, B. Jannier, Y. Le Bihan, O. Dubrunfaut, O. Meyer, and L. Pichon, "Direct and inverse modeling of a microwave sensor determining the proportion of fluids in a pipeline," *IEEE Trans. Magn.*, vol. 45, no. 3, pp. 1510–1513, Mar. 2009.
[16] T. N. Kapetanakis, I. O. Vardiambasis, M. P. Ioannidou, and A. Maras, "Neural network modeling for the solution of the inverse loop antenna radiation problem," *IEEE Trans. Antennas Propag.*, vol. 66, no. 11, pp. 6283–6290, Nov. 2018.
[17] Y. Sharma, H. H. Zhang, and H. Xin, "Machine learning techniques for optimizing design of double T-shaped monopole antenna," *IEEE Trans. Antennas Propag.*, vol. 68, no. 7, pp. 5658–5663, Jul. 2020.
[18] A. Gupta, E. A. Karahan, C. Bhat, K. Sengupta, and U. K. Khankhoje, "Tandem neural network based design of multiband antennas," *IEEE Trans. Antennas Propag.*, vol. 71, no. 8, pp. 6308–6317, Aug. 2023, doi: 10.1109/TAP.2023.3276524.
[19] J. P. Jacobs, "Accurate modeling by convolutional neural-network regression of resonant frequencies of dual-band pixelated microstrip antenna," *IEEE Antennas Wireless Propag. Lett.*, vol. 20, no. 12, pp. 2417–2421, Dec. 2021, doi: 10.1109/LAWP.2021.3113389.
[20] A. Gehani and D. A. Pujara, "Predicting the return loss performance of a HEXA-band PIFA using ANFIS," *Microw. Opt. Techn. Lett.*, vol. 57, no. 9, pp. 2072–2075, Sep. 2015.
[21] L.-Y. Xiao, W. Shao, F.-L. Jin, B.-Z. Wang, and Q. H. Liu, "Inverse artificial neural network for multiobjective antenna design," *IEEE Trans. Antennas Propag.*, vol. 69, no. 10, pp. 6651–6659, Oct. 2021.
[22] S. Koziel and A. Bekasiewicz, "Rapid dimension scaling for notch-frequency redesign of UWB band-notch antennas," *J. Electromagn. Waves Appl.*, vol. 30, no. 17, pp. 2280–2292, Nov. 2016.
[23] Y. Sharma, X. Chen, J. Wu, Q. Zhou, H. H. Zhang, and H. Xin, "Machine learning methods-based modeling and optimization of 3-D-printed dielectrics around monopole antenna," *IEEE Trans. Antennas Propag.*, vol. 70, no. 7, pp. 4997–5006, Jul. 2022, doi: 10.1109/TAP.2022.3153688.
[24] Y. Xiao, K. W. Leung, K. Lu, and C.-S. Leung, "Mode recognition of rectangular dielectric resonator antenna using artificial neural network," *IEEE Trans. Antennas Propag.*, vol. 70, no. 7, pp. 5209–5216, Jul. 2022, doi: 10.1109/TAP.2022.3146860.
[25] S. Koziel, A. Bekasiewicz, and L. Leifsson, "Rapid EM-driven antenna dimension scaling through inverse modeling," *IEEE Antennas Wireless Propag. Lett.*, vol. 15, pp. 714–717, 2016.
[26] M. N. Qureshi, M. K. Shahid, M. I. Tiwana, M. Haddad, I. Ahmed, and T. Faisal, "Neural networks for energy-efficient self optimization of Enodeb antenna tilt in 5G mobile network environments," *IEEE Access*, vol. 10, pp. 61678–61694, 2022, doi: 10.1109/ACCESS.2022.3181595.
[27] Z. Ž. Stanković, D. I. Olćan, N. S. Dončov, and B. M. Kolundzija, "Consensus deep neural networks for antenna design and optimization," *IEEE Trans. Antennas Propag.*, vol. 70, no. 7, pp. 5015–5023, Jul. 2022, doi: 10.1109/TAP.2021.3138220.
[28] S. Mishra, R. N. Yadav, and R. P. Singh, "Directivity estimations for short dipole antenna arrays using radial basis function neural networks," *IEEE Antennas Wireless Propag. Lett.*, vol. 14, pp. 1219–1222, 2015.

[29] G. Gosal, E. Almajali, D. McNamara, and M. Yagoub, "Transmit array antenna design using forward and inverse neural network modeling," *IEEE Antennas Wireless Propag. Lett.*, vol. 15, pp. 1483–1486, 2016.
[30] L. Yuan, X.-S. Yang, C. Wang, and B.-Z. Wang, "Multibranch artificial neural network modeling for inverse estimation of antenna array directivity," *IEEE Trans. Antennas Propag.*, vol. 68, no. 6, pp. 4417–4427, Jun. 2020.
[31] C. Cui, W. T. Li, X. T. Ye, P. Rocca, Y. Q. Hei, and X. W. Shi, "An effective artificial neural network-based method for linear array beam-pattern synthesis," *IEEE Trans. Antennas Propag.*, vol. 69, no. 10, pp. 6431–6443, Oct. 2021.
[32] Y. Gong, S. Xiao, and B.-Z. Wang, "An ANN-based synthesis method for nonuniform linear arrays including mutual coupling effects," *IEEE Access*, vol. 8, pp. 144015–144026, 2020, doi: 10.1109/ACCESS.2020.3013880.
[33] Y. Jiao, Q. Zhu, R. Ni, and Q. S. Cheng, "A multisurrogate-assisted optimization framework for SSPP-based mmWave array antenna," *IEEE Trans. Antennas Propag.*, vol. 71, no. 4, pp. 2938–2945, Apr. 2023, doi: 10.1109/TAP.2023.3240239.
[34] M. Montaser and K. R. Mahmoud, "Deep learning based antenna design and beam-steering capabilities for millimeter-wave applications," *IEEE Access*, vol. 9, pp. 145583–145591, 2021, doi: 10.1109/ACCESS.2021.3123219.
[35] M. Gustafsson, D. Tayli, C. Ehrenborg, M. Cismasu, and S. Nordebo, *Antenna Current Optimization Using MATLAB and CVX*, Forum for Electromagn. Res. Methods Appl. Technol., Shizuoka, Japan, 2016.
[36] J. L. Volakis and K. Sertel, *Integral Equation Methods for Electromagnetics*. Chennai, India: Scitech, 2012.
[37] C. A. Balanis, *Antenna Theory: Analysis and Design*. Hoboken, NJ, USA: Wiley, 2016
[38] J. Mautz and R. Harrington, "Modal analysis of loaded N-port scatterers," *IEEE Trans. Antennas Propag.*, vol. AP-21, no. 2, pp. 188–199, Mar. 1973.
[39] A. Yee and R. Garbacz, "Self- and mutual-admittances of wire antennas in terms of characteristic modes," *IEEE Trans. Antennas Propag.*, vol. AP-21, no. 6, pp. 868–871, Nov. 1973.
[40] R. Storn and K. Price, "Minimizing the real functions of the ICEC'96 contest by differential evolution," in *Proc. IEEE Conf. Evol. Comput.*, May 1996, pp. 842–844.
[41] A. Clemente, C. Jouanlanne, and C. Delaveaud, "Analysis and design of a four-element superdirective compact dipole antenna array," in *Proc. 11th Eur. Conf. Antennas Propagat. (EUCAP)*, 2017, pp. 2700–2704, doi: 10.23919/EuCAP.2017.7928259.
[42] "MVGworld." [Online]. Available https://www.mvgworld.com

ABDELLAH TOUHAMI (Student Member, IEEE) received the bachelor's degree in electronics from Ibn Zohr University, Agadir, Morocco, in 2017, and the M.Cs. degree in control, computer science, signals, and systems from Cadi Ayyad University Marrakech, Morocco, in 2019. He is currently pursuing the Ph.D. degree with the Institute of Electronics and Digital Technologies, Rennes, France. His research interests include superdirective antennas, electrically small antennas, network characteristics modes, and RF circuits design.

SYLVAIN COLLARDEY graduated in electronics and telecommunication engineering from the University of Rennes 1, France, in 1998. He received the Ph.D. degree in telecommunication from the University of Rennes 1 in 2002, where he is currently an Associate Professor and involved as a Researcher with the Antennas and Microwaves Group, Electronics and Digital Technologies of Rennes. He has published more than hundred revue papers and conference communications. His current research interests include the characterization and development of small antennas, EBG materials and metamaterials, and RFID.

ALA SHARAIHA (Senior Member, IEEE) received the Ph.D. and Habilitation á Diriger la Recherche degrees in telecommunication from the University of Rennes 1, France, in 1990 and 2001, respectively, where he is currently a Full Professor and the Co-Head of the Antennas and Microwave Devices Department, IETR Research Laboratory (Institute of Electronics and Telecommunications in Rennes). He has graduated/mentored more than 42 Ph.D. students/postdocs and coauthored with them. He has authored or coauthored more than 500 journal and conference papers, concerning antenna theory, analysis, design, and measurements. He holds 14 patents. His published works have been cited over 2400 times in Google Scholar. His current research interests include small antennas, broadband and UWB antennas, reconfigurable antennas, printed spiral and helical antennas, and antennas for mobile communications. He is a Reviewer of the IEEE TRANSACTIONS ON ANTENNAS AND PROPAGATION, IEEE ANTENNAS AND WIRELESS PROPAGATION LETTERS, the *IET Letters*, and the *IET Microwave Antennas Propagation*. He was the Conference Chairman of the 11th International Canadian Conference Antenna Technology and Applied Electro-Magnetics, Saint-Malo, France, 2005. He is presently a French Delegate Member of the European Association on Antennas and Propagation (EuRAAP) and a member of the small antennas working group of EuRAAP.